Materials Chemistry and Physics 302 (2023) 127686

Contents lists available at ScienceDirect

Materials Chemistry and Physics

journal homepage: www.elsevier.com/locate/matchemphys

Hydrophobic-oleophilic surfaces based on chemical modification of nanoporous alumina

Pilar Formentín, Laura K. Acosta, Lluís F. Marsal *

Departament d'Enginyeria Electrònica, Elèctrica i Automàtica, Universitat Rovira i Virgili, Avinguda Països Catalans 26, 43007, Tarragona, Spain

HIGHLIGHTS

- Fabrication and characterization of nanoporous anodic alumina structures.
- Perfluorooctyl functionalization of nanoporous surfaces.
- Influence of topography and surface chemistry on the wettability of nanoporous alumina substrates.
- Contact angle measurements using water and non-polar solvents.
- Surface energy of nanoporous anodic alumina surfaces calculated by "three-liquid acid-base procedure".

GRAPHICAL ABSTRACT

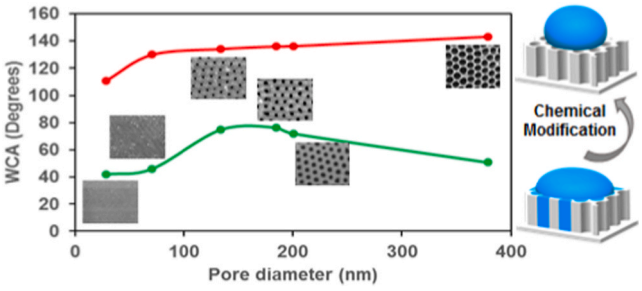

ARTICLE INFO

Keywords:
Nanoporous anodic alumina
Surface modification
Wettability
Hydrophobicity
Oleophilic surface

ABSTRACT

Hydrophobic/oleophilic nanoporous anodic alumina substrates were fabricated by two-step anodization method following of chemical modification with 1H, 1H, 2H, 2H-perfluorooctyltrichlorosilane (FOTS). Surface morphology was characterized using a scanning electron microscopy. The influence of the topography and the pore size of the surface in the contact angle measurements with different solvents have been studied. The water repellence capacity of the nanoporous anodic alumina structure as fabricated depends on pore diameter but, there is a critical value of pore size beyond which the water contact angle decrease. After chemical modification of the surface, this effect is not observed. The porous topography of the material is not an advantage for the oleophibicity. The CA values for the non-porous surface using different solvents are lower than the structured surface.

The results obtained in this study can be used to desire wettability properties. Modified NAA exhibit hydrophobicity and at the same time permeability for solvents with low surface tension.

1. Introduction

Wettability is a surface property of a solid material used in a variety of field in industrial applications and also in daily [1–6]. Two factors can regulate this property of the materials: one is the surface topology and the other is the chemical component of the surface. The surface topology can be explained by the classical theoretical models attributed to Wenzel [7], Cassie [8] and derivatives [9,10]. Wenzel state is a complete wetting state, the space between the surface protrusions on the surface is totally wetted with liquid (Fig. 1a). In the Cassie state, the liquid droplet cannot immerse into the structure. The liquid is only on the top of the rough surface due to the air fraction trapped at the bottom between the

* Corresponding author.
E-mail address: lluis.marsal@urv.cat (L.F. Marsal).

https://doi.org/10.1016/j.matchemphys.2023.127686
Received 22 November 2022; Received in revised form 23 March 2023; Accepted 27 March 2023
Available online 12 April 2023

liquid droplet and the surface (Fig. 1b). The contact angle (CA) is utilized as a measure of wetting between a liquid and a solid surface and can be assessed directly by measuring the angle formed between the solid and the tangent to the drop surface. The CA of water in the Wenzel and Cassie states can be calculated using the following equations:

$$\cos\theta_w = r\cos\theta_Y \quad (1)$$

$$\cos\theta_{CB} = (\cos\theta_Y + 1)f - 1 \quad (2)$$

where θ_Y is the Young's CA of a smooth surface [11], r is the area ratio of structured surface to planar surface ($r \geq 1$), θ_w is CA in the Wenzel state, θ_{CB} is the CA in the Cassie state and, f is the surface fraction of the droplet that is in contact with the surface.

In some cases, when the droplet is placed on structured surfaces, the liquid partially enters into the structure allowing the liquid droplets stick to the surface. This state is called intermediate state and have been studied by different authors [12,13] (Fig. 1c).

Wettability can be modified by creating a rough micro- or nanostructure [14–19], or by modifying the substrate with a layer of chemical coating [20–26]. By design and modifying with a particular chemical modification, some surfaces simultaneously can be showing different behaviour. Porous hydrophobic and oleophilic materials (PHOMs) are interesting in microfluidics [27,28], oil/water separation [29–31], oil cleaning or oil droplet manipulation [32,33]. This type of materials have been demonstrate to be good candidates for cleaning up oil spills, which have increased in the last decades and it have caused damages to the environment and also to the society [34]. PHOMs have the option to eliminate an oil layer from the water surface.

In the last decade, several studies have been focused on fabrication of hydrophobic surfaces on metal, such as aluminium. Preparation of hydrophobic surface with micro- or nanostructures is of interest to improve the surface performance of aluminium. Many techniques have been reported to obtain super- and hydrophobic surfaces on aluminium [22, 35–38]. The anodization method is one of the methods in preparing micro and nanostructures, such as nanoporous anodic alumina (NAA), for large-scale applications. This technique allows controlling the surface morphology by anodization time or voltage.

Nanoporoous anodic alumina (NAA) is an attractive material for surface engineering due to because of its cost-effective and highly controlled fabrication process such as interpore distance and diameter of pores and, good thermal stability. NAA has been used in a different range of applications [39–43]. Moreover, the high content of hydroxyl groups on the surface make easier the functionalization of the material, which improve the properties of the alumina for different applications such as biocompatibility for cell culture, tissue engineering or drug delivery [44–49].

It is well-know the fabrication of porous materials with selective wettability by chemical functionalization with alkyl or fluorine groups. Herein, we prepare NAA chemically modified using a hydrophobic self-assembled monolayer (1H, 1H, 2H, 2H,-perfluorooctyltrichlorosilane, FOTS), to give a lower surface energy while maintaining the surface topography [21,23,50,51]. The non-polar nature of fluorinated alkanes awards range properties, such as water repellence.

In this paper, surface nanostructure is modified in order to improve the hydrophobicity of the NAA and, we have studied the simultaneous oleophilicity of the material with different liquids after functionalization. FOTS present fluorinated groups, which reduces the surface energy with the material and can self-assemble on surfaces with hydroxyl groups such as the NAA samples. Our results demonstrate that with a particular functionalization the same material can be hydrophobic and oleophilic at the same time. The topography of the surface and in specific the pore diameter and the porosity of the sample play a role in the wettability of the material. Another parameter to consider is the surface energy. It have also been calculated by the van Oss-Good model, which consider acid-base interactions.

This type of surfaces are more studied recently because of their applications in oil/water separation, anti-oils coatings, oil droplet manipulation or oil capture.

2. Experimental section

2.1. Fabrication of nanoporous anodic alumina (NAA)

Nanoporous anodic alumina was fabricated from high purity 99.999% aluminium foils (Goodfellow, Cambridge Ltd.) using a two-step anodization process in different acids [52–54]. The first anodization was performed at 40 V in 0.3 M oxalic acid ($H_2C_2O_4$) solution at 5 °C for 20 h or 1% phosphoric acid (H_3PO_4) at 195 V for 20 h at −5 °C. After removing porous alumina by a wet chemical etching in a mixture of 0.4 M phosphoric acid (H_3PO_4) and 0.2 M chromic acid (H_2CrO_4) at 70 °C, a second step was carried out until a total charge of 80 C per sample used in the anodization. The anodic oxidation of aluminium can result NAA of 20 μm thickness with pore diameters from 25 nm to 130 nm. A wet chemical etching in 5 wt % phosphoric acid at 35 °C was applied to widened the pore size and it increase with the time prolongation. Etching times of 20, 40 and 95 min were selected.

2.2. Surface characterization

NAA substrates morphology were analyzed by scanning electron microscopy using a FEI Quanta 600 environmental scanning electron microscope (ESEM) (Hillsboro, OR, USA) operated in low vacuum at an accelerating voltage between 15 and 20 KeV.

2.3. Chemical modification of NAA surfaces

All the NAA substrates were treated with 1H, 1H, 2H, 2H,-perfluorooctyltrichlorosilane (FOTS) (CAS: 78560-45-9, Alfa Aesar, Germany). The same approach as in previous work was employed [55]. In brief, 40 μl of FOTS was dropped into 40 ml of n-hexane. Each NAA sample was placed inside the FOTS-hexane solution for 1h with gentle agitation. The substrates were then take out of the solution, rinsed with hexane and place in an oven at 110 °C for 1h. The samples were rinsed with acetones and left to dry.

2.4. Contact angle measurements

Contact angles (CA) were measured using a drop shape analysis system under ambient conditions applying solvent droplets of about 3 μl. The average CA value was obtained by measuring 9 times at three

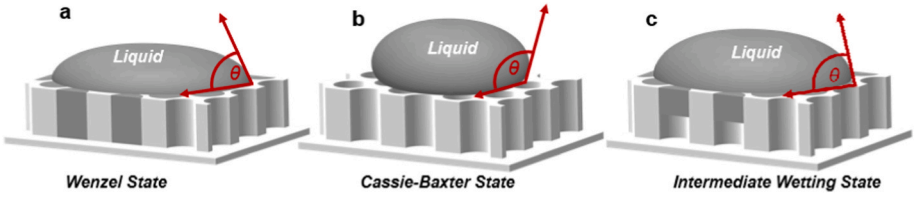

Fig. 1. Classical theoretical models. Schematic representation of a liquid droplet on non-planar surface: a) Wenzel's model, b) Cassie's model and c) Intermediate state.

different positions for each sample.

2.5. Infrared spectrometry

Fourier transform infrared (FTIR) spectroscopy was used to characterize the surface after chemical surface modification. FTIR spectra were obtained using a Jasco FT/IR-6700 Infrared Spectrometer in transmittance mode. Background spectra and sample spectra were recorded over the range of 500–2500 cm^{-1} at a resolution of 4 cm^{-1} and averaging 64 scans. Data were analyzed using Spectra Manager™ Suite Spectroscopy Software.

2.6. Energy dispersive X-ray spectroscopy (EDX)

Nanoporous anodic alumina subtrates after chemical modification were analyzed by energy-dispersive X-ray spectroscopy using a detector coupled to FEI Quanta 600 environmental scanning electron microscopy.

3. Results and discussion

3.1. Fabrication and characterization of nanoporous anodic alumina

The nanoporous anodic alumina was fabricated in a controllable process using the two-step anodization method as we describe previously in experimental section. The pore diameter were tuned by varying etching conditions (Table 1). Fig. 2 shows top view ESEM images of nanoporous alumina surfaces of 20 μm thick NAA layers grown from oxalic and phosphoric electrolytes. The anodic oxidation of aluminium in oxalic acid can result in the pore diameters from 25 nm to 30 nm, which can be widened after etching treatment. When the electrolyte used in the anodization step is phosphoric acid, the pore diameter obtained is from 130 nm to 135 nm and it can be growth with different etching times until 370 nm.

After ESEM characterization of the samples, we can observe that the pore size, the pore wall thickness and the porosity are affected by the etching parameters, while keeping the interpore distance remains constant using the same electrolyte (Table 2).

3.2. Wettability of NNA surfaces

The wettability of the fabricated nanoporous surfaces was characterized by contact angle measurements with 3 μl of water droplets. We also analyzed the wettability on non-porous flat alumina substrate. In this case, the surface is hydrophilic with a water contact angle (WCA) of 64.25°, which is lower than the electropolished Al surface (85.01°) and different to the values reported previously [50]. It may be come from different structural features due to different conditions during the preparation of the surface and it affect the WCA values. Herein, the non-porous alumina surface was obtained at 40 V in 0.3 M oxalic acid solution at 5 °C during 15 s.

Table 1
Etching conditions for preparation nanoporous anodic alumina substrates by anodization technique.

	Electrolite	Voltage (V)	Temperatura (°C)	Etching Time (min)
NAA-O-NE	0.3 M Oxalic acid	40	5	0
NAA-O-E20	0.3 M Oxalic acid	40	5	20
NAA-P-NE	1% Phosphoric acid	195	−5	0
NAA-P-E20	1% Phosphoric acid	195	−5	20
NAA-P-E40	1% Phosphoric acid	195	−5	40
NAA-P-E95	1% Phosphoric acid	195	−5	95

The degree of wettability of NAA can be determinated by the contact angle and, to understand the behavior of contact angle on nanoporous surfaces, pore size should be considered. It is well-known that the pore diameter and the porous alumina thickness influence on the wetting [13,56–58]. In Fig. 3, the WCA as a function of the pore diameter for the fabricated NAA structures is plotted. As the figure shows, increases in pore size lead to changes in wettability surface. We observe that there is a critical pore diameter from which WCA falls down. The pore walls become too thin with increasing etching time, and then it cannot support the water droplet. It spreads easily and the hydrophobicity of the surface decrease. Similar results are reported in previously works [55,59].

When the geometrical parameters pore diameter and interpore distance are modified, porosity is also altered. For different porosity values will be different solid-liquid contacts and, the geometry of water droplet on the porous surface will be different.

Herein, the porosity value has been calculated from the surface topography from ESEM images using ImageJ software, by counting the percentage of pixels whose intensity is below a set threshold. The porosity is the "surface porosity" of the sample that is the area fraction occupied by depressions. Fig. 4 illustrates the WCA values at different porosity for all samples. The results show that no correlation between porosity and contact angle was found.

3.3. Chemical modification and wettability properties of NAA substrates

Chemical modification of the nanoporous anodic alumina structures offers a solution for the obtaining of hydrophobic surfaces. Herein, NAA surfaces were modified utilizing a hydrophobic surface coupling agent (1H,1H,2H,2H-perfluorooctyltrichlorosilane (FOTS)), in order to improve the hydrophobic properties of the material. The surface property of the NAA-FOTS was characterized by measuring contact angle with water (WCA). FOTS increase the water repellence of the substrates because it hydrophobic termini with fluorinated tail groups and reduce the surface energy with the substrate. This silane can self-assemble on any surface with hydroxyl groups such as aluminum oxide (Al_2O_3).

A direct comparison of untreated and modified non-porous alumina and NAA-P-E95 is presented in Fig. 5. The surface of non-porous alumina is hydrophilic and, as we mentioned before, a surface modification with FOTS leads to an increased hydrophobicity. This increase is observed also in the NAA structure. The combination of the porous alumina surface and chemical modification with a silane with fluorine groups allow the fabrication of hydrophobic aluminum oxide surfaces.

Fig. 6 exhibits that there is a critic pore diameter from which WCA falls down as we explained previously. After surface modification with the fluorosilane reagent, all the nanostructures exhibit a change toward hydrophobic surfaces, which present CA values higher than 90 °C. The WCA values do not follow the pore diameter trend as the given in Fig. 3. It is possible that hydrophobic tails in FOTS prevent water entrance into the pores and the water does not experience in the same way the influence of the surface's topography as is explained in a previous work [55]. WCA values for NAA-FOTS are higher than for non-porous-FOTS surface, so we can confirm that the porous are required to obtain high hydrophobicity in alumina.

FTIR spectra of aluminium, non-porous alumina and NAA fabricated from oxalic acid before and after chemical modification is shown in Fig. 7. NAA samples show characteristic peaks for Al–O bonds from 1400 to 1600 cm^{-1}. The peaks at 1124, 1144, 1212 and 1239 $cm^{-1}$for the NAA modified surface are attributed to the CF_2 groups. The bands for CF_3 group are in the range of 1110–1350 $cm^{-1}$and is difficult to distinguish it overlaps with the CF_2 bands. We confirm that the hydrophilic property of NAA is modified by FOTS to form hydrophobic surfaces in the FTIR analysis shown in Fig. 7 but, it do not allow a quantitative comparison of the functionalization groups on the different samples.

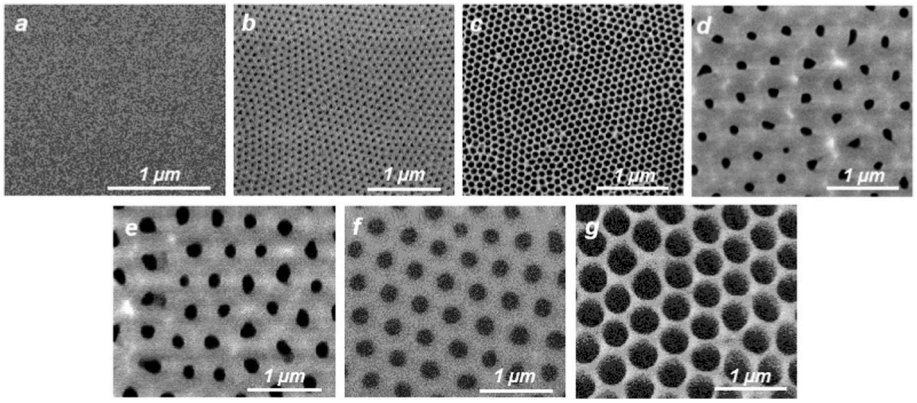

Fig. 2. Morphological analysis of Nanoporous Anodic Alumina. Top view ESEM images of nanoporous anodic alumina with different pore size. a) Non-porous alumina, b) NAA-O-NE, etching time 0 min, pore diameter = 28.01 ± 2.54 nm, c) NAA-O-E20, etching time 20 min, pore diameter = 70.15 ± 5.87 nm, d) NAA-P-NE, etching time 0 min, pore diameter = 133.73 ± 13.34 nm, e) NAA-P-E20, etching time 20 min, pore diameter = 184.47 ± 19.34 nm, f) NAA-P-E40, etching time 40 min, pore diameter = 200.30 ± 10.21 nm, g) NAA-P-E95, etching time 95 min, pore diameter = 378.90 ± 12.10 nm.

Table 2
Geometrical parameters of nanoporous anodic alumina substrates and WCA values.

	d_{pore} (nm)	d_{interp} (nm)	Porosity (%)	WCA (°)
NAA-O-NE	28.01 ± 2.54	101.25 ± 4.20	16.55 ± 4.18	42.10 ± 7.83
NAA-O-E20	70.15 ± 5.87	103.81 ± 5.68	50.24 ± 1.51	46.12 ± 5.65
NAA-P-NE	133.73 ± 13.34	453.78 ± 17.25	8.35 ± 0.96	74.81 ± 2.21
NAA-P-E20	184.47 ± 19.34	454.15 ± 15.52	17.23 ± 0.64	76.37 ± 3.35
NAA-P-E40	200.30 ± 10.21	459.22 ± 8.37	26.0 ± 1.21	71.93 ± 6.65
NAA-P-E95	378.90 ± 12.10	455.21 ± 3.74	56.81 ± 0.83	50.75 ± 4.15

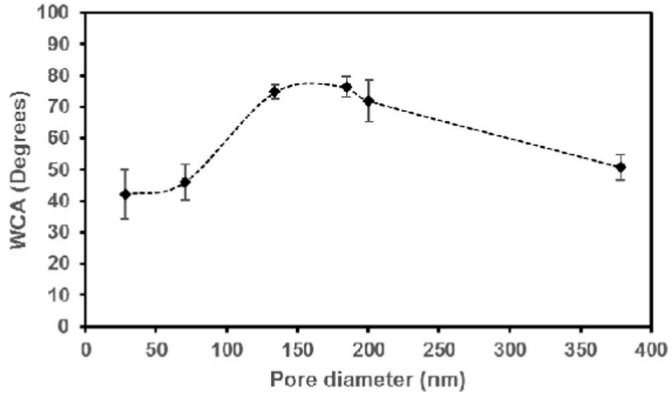

Fig. 3. Water contact angle versus pore diameter. WCA measurements as a function of pore diameter of NAA substrates obtained with different anodizing parameters.

Fig. 8 shows the EDX spectra of NAA surfaces from different electrolyte etching after chemical modification. It can be seen that the NAA-FOTS consist of O and Al from Al_2O_3 and F from the hydrophobic coupling agent (FOTS). The minimum C and P on the surface might be from the electrolyte residual from the anodization step or the etching to widen the pore size. The ratio of aluminium to oxygen in Al_2O_3 calculated from EDX data is 1.09 for NAA-O-E20 and 1.12 for NAA-P-E95, which correspond to the alumina value (1.12).

3.4. Oleophilic performance of chemically modified NAA substrates

Some porous materials show, simultaneously, hydrophobicity and oleophibicity after designing and modifying chemical chains on the

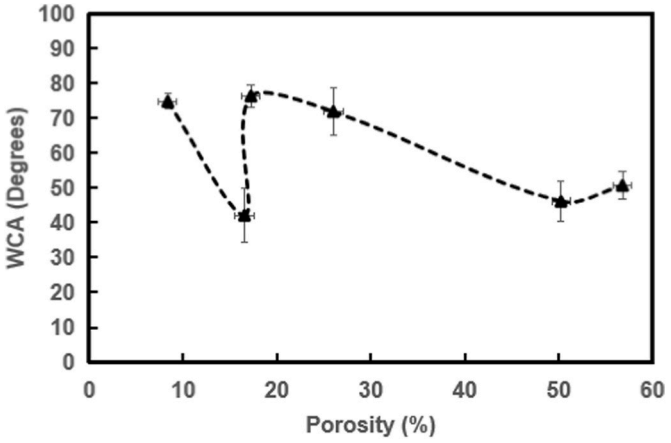

Fig. 4. Water contact angle versus surface porosity. WCA as a function of the surface porosity for NAA structures.

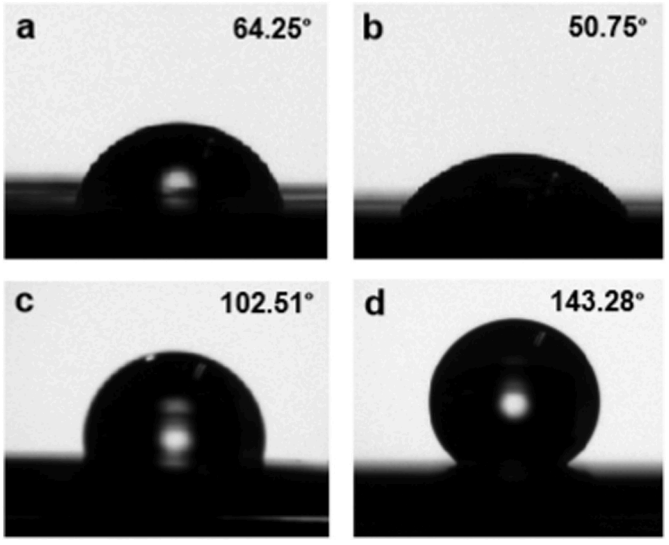

Fig. 5. Comparison of untreated and modified non-porous alumina and NAA. Images of 3 μl water drops deposited on: a) Non-porous alumina, b) Nanoporous anodic alumina NAA-P-E95, c) Non-porous alumina after modification with FOTS, d) Nanoporous anodic alumina NAA-P-E95 after modification with FOTS.

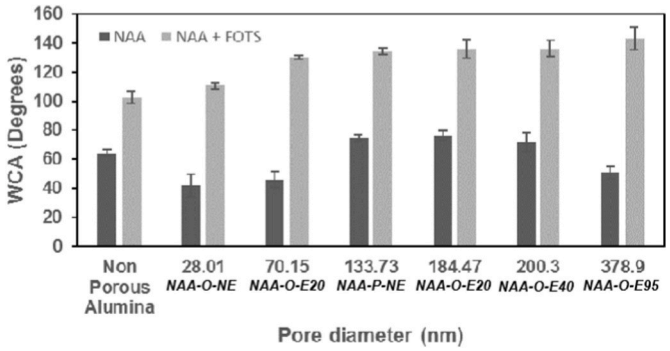

Fig. 6. Comparison of WCA value of nanoporous structures before and after chemical modification versus pore diameter. WCA measurements as a function of pore diameter of NAA substrates before and after chemical modification with FOTS.

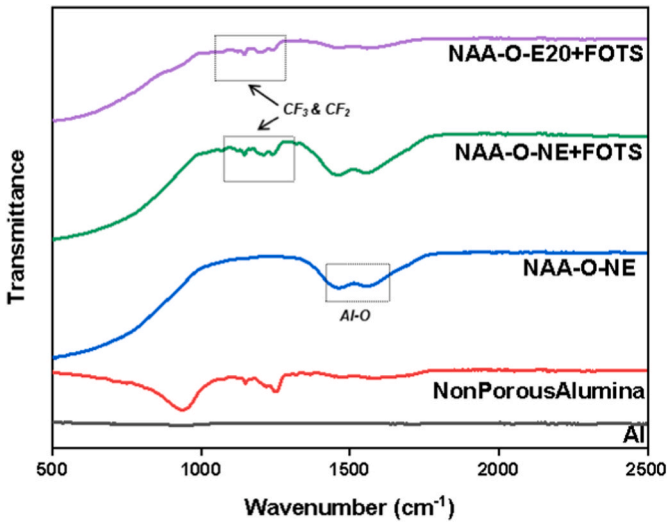

Fig. 7. Infrared spectrometry. FTIR spectra for aluminium, non-porous alumina, NAA-O-NE and NAA-FOTS with different pore diameter.

surface. Organic materials and most solvents are considered as low energy materials with respect to their surface energies (Table 3), whereas inorganic materials, such as aluminium dioxide, are referred as high-energy materials. In order to analyzed the oleophilic behaviour of the modified nanoporous anodic alumina, contact angle on the NAA-FOTS was measured using organic solvents with low surface tension (Table 4).

Low-energy liquids spread on high-energy surfaces such as alumina oxide. This effect is observe when we compare CA values from the same surface using different liquids like water and decane or chloroform. The water occupies the top of the nanopores and solvents with low surface tension wet or even can fill the pore walls.

The CA values for the non-porous surface are lower than the structured surface for almost all the liquids. Therefore, we can say that the porous topography of the material is not an advantage for the oleophibicity of this oxide substrate.

The contact angle values versus the pore diameter is shown in Fig. 9. The WCA increase with the increasing of the pore diameter but no correlation was found between topography and wettability in the case of chloroform or decane. The droplet of non-polar solvent spread out on the NAA surface and is partly absorbed by the substrate. These solvents present stronger interactions with the chemical groups of the surface (oxalate and phosphate groups and $–CF_2$-CF_3) which can explain the contact angle values obtained. These interactions also exist with water but, the high surface tension ($\gamma = 71.8$) leads to high CA values.

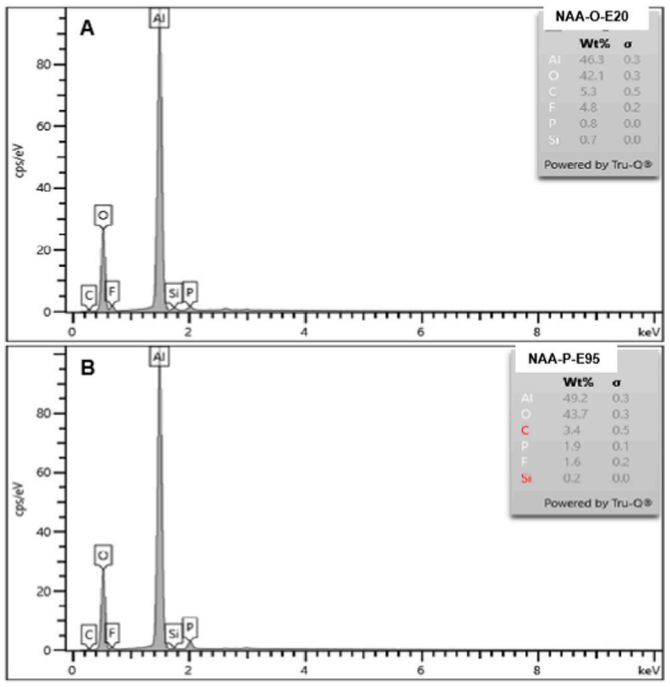

Fig. 8. Energy dispersive X-ray spectroscopy. EDX spectra of NAA substrates after chemical modification.

Table 3
Surface tension and its components at 20 °C [63].

	γ^{LW}	γ^{-}	γ^{+}	γ^{T}
Water	21.8	25.5	25.5	71.8
N-Decane	23.83	0	0	23.83
Chloroform	27.2	0	3.8	27.2

From these results, NAA-FOTS structures can be simultaneously considered hydrophobic (CA > 90 °C) and oleophilic (CA < 90 °C) with low surface tension liquids (Fig. 10).

3.5. Surface energy of NAA structures with different liquids

The energy related to the intermolecular forces at the interface between two media is defined as surface energy. It can be explained as the energy necessary per unit area to increase the size of the surface (N/m). If the molecular interactions are stronger, surface energy will be higher and, it will generally cause good wetting. On the other hand, poor wetting will be caused by a surface with a low energy. This is due to the surface is not able of forming strong bonds and, there is low energetic reward for the liquid to break bulk bonding in favour of interacting with the surface (Fig. 11).

The most common way to measure surface energy is through contact angle, which is measured with several liquids. Another factor to consider is the surface tension of the liquid, as well as the type of interactions between the liquid and solid. Low surface energy causes poor wetting and a high contact angle (hydrophobic surface), while high surface energy causes good wetting and low contact angle value (hydrophilic surface).

With the contact angle values and knowing the surface tension of the solvents, the surface energy can be calculated.

In this work, the surface energy of the NAA-FOTS samples have been calculated from a “three-liquid acid-base procedure” developed by van Oss et al. [60–62]. This model considers acid-base interactions. It combines polar and dispersive interactions in one term and is defined by the following equation:

Table 4
Contact angle values of three probe liquids on NAA-FOTS surfaces and the calculated surface energies (mN/m).

	Non Porous Alumina	NAA-O-NE	NAA-O-E20	NAA-P-NE	NAA-P-E20	NAA-P-E40	NAA-P-E95
CONTACT ANGLE							
Water	102.51 ± 4.06	110.59 ± 2.21	129.90 ± 1.28	134.16 ± 2.29	136.06 ± 6.57	136.30 ± 5.52	143.28 ± 7.75
N-Decane	56.31 ± 1.76	58.96 ± 4.21	80.12 ± 0.44	66.11 ± 2.75	61.06 ± 1.48	62.81 ± 0.53	90.99 ± 0.45
Chloroform	53.81 ± 1.64	53.82 ± 1.81	71.48 ± 0.38	60.81 ± 0.35	64.20 ± 1.49	66.42 ± 1.75	85.35 ± 4.34
SURFACE ENERGY							
γ_{AB}	16.5	13.71	13.22	17.1	14.18	13.43	10.1
γ_{LW}	14.41	13.68	8.17	11.75	13.11	12.64	5.75
γ	2.1	0.02	5.04	5.34	1.06	0.79	4.35
γ_{+}	1.24	9.11E-05	2.68	4.92	2.81	2.46	3.73
γ_{-}	0.89	1.43	2.37	1.44	0.1	0.06	1.26

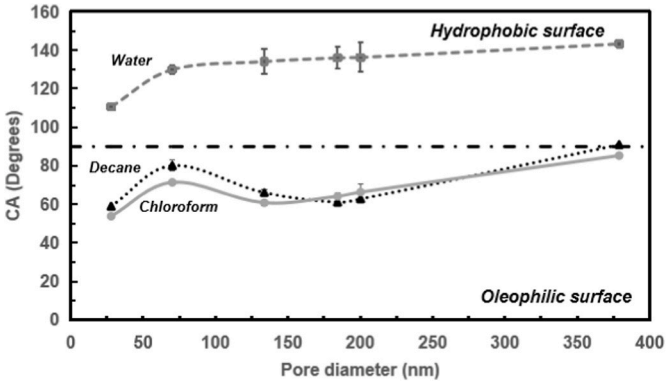

Fig. 9. Oleophilic behaviour of the modified NAA. Contact angle values versus pore diameter for different solvents on NAA-FOTS.

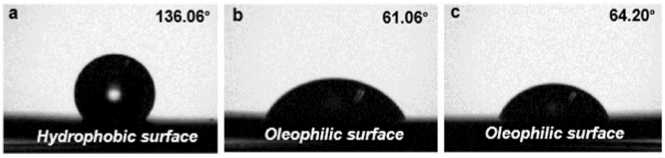

Fig. 10. Hydophobic/Oleophilic surfaces. Images of (a) water, (b) decane and (c) chloroform droplet on chemical modified NAA-P-E20 nanostructure with a porosity of 17.23 ± 0.64%.

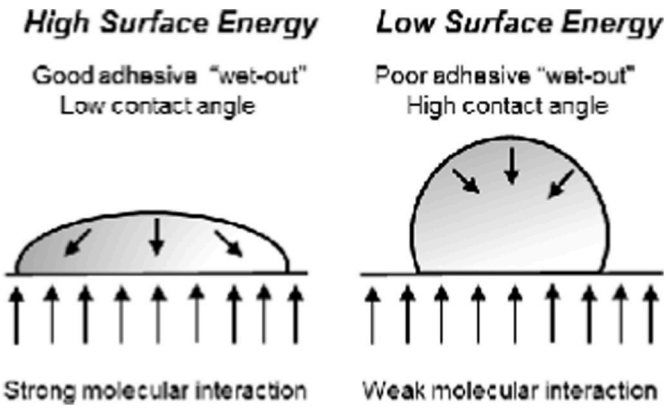

Fig. 11. Surface energy. A basic depiction of surface energy showing molecular interactions between a liquid and a surface.

$$\gamma_L^T(1+\cos\theta) = 2\{(\gamma_S^{LW}\gamma_L^{LW})^{0.5} + (\gamma_S^{+}\gamma_L^{-})^{0.5} + (\gamma_S^{-}\gamma_L^{+})^{0.5}\} \quad (3)$$

Where γ^T, γ^{LW}, γ^{+} and γ^{-} mean the total Lifshitz-van der Waals (dispersive), lewis acid and base surface components. The subscripts S and L refer to the solid surface and probe liquid. The final γ^T of solid is obtained by

$$\gamma^T = \gamma^{LW} + \gamma^{AB} \quad (4)$$

Where γ^{AB} is defined by $2(\gamma_S^{+}\gamma_S^{-})^{0.5}$

Water, decane and chloroform are chosen as three probe liquids in this work. Using the surface tension data provide in Table 3 into equations (1) and (2) and, the resultant contact angles summarize on Table 4, we calculated the surface energy of NAA structures after chemical modification with FOTS (Table 4).

As known, the surface energies of the liquid, substrate and of the interface between them determine the wettability and the contact angle values. Another factor to consider is the surface topography. We have observe that in NAA-FOTS substrates, the CA increase with increasing pore diameter. As we expected, and we illustrate in Table 4, the sample with the largest diameter (NAA-P-E95) is the one with the highest contact angle and the lowest surface energy. The adhesion of the liquid to the surface is better in flat alumina that in NAA structures and, because that the highest surface energy obtained in the case of the non-structure alumina.

The surface energy has also calculated for the rest of the samples. We have noticed not correlation between pore diameter and surface energy as is show in Table 4. If we compare samples fabricated by the same electrolyte, we observe decreasing of surface energy with increase of pore diameter as in NAA-O-NE & NAA-O-E20 fabricated from oxalic acid and NAA-P-NE & NAA-P-E95 fabricated from phosphoric acid. It seems that the residual surface groups on the sample, as oxalate or phosphate, affects in the surface energy measured. On the other hand, we observe an effect of the porosity on the surface energy measurements. Results

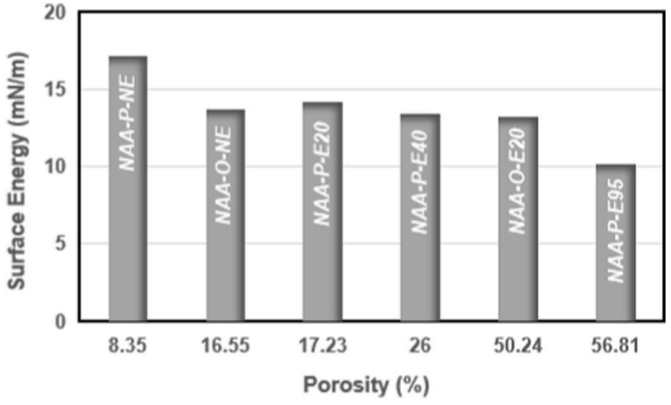

Fig. 12. Surface energy of modified NAA. Surface energy as a function of porosity of NAA-FOTS substrates.

indicate higher energy for samples with less porosity (Fig. 12).

4. Conclusions

Nanoporous anodic alumina structures with diverse topography were fabricated by two-step anodization process in oxalic or phosphoric acid. Two different surface modification methods are analyzed: the well-defined nanotopogaphies and surface chemistry. We have studied how these parameters influence on the wettability and in the surface energy of nanoporous anodic alumina structures, which have been calculated following a theoretical model based on acid base interactions. Contact angle measurements shows that the surface after chemical modification exhibits repellence towards water with a WCA higher than 90° and permeability towards non polar oils. The hydrophobicity increase when the increasing of the pore diameter and it cause poor wetting and low surface energy. In the case of the oleophilic feature, the best result is obtain with non-porous structure. Surface energy of the NAA-FOTS structures have been calculated from "three liquid acid-base procedure". There are not correlation between pore diameter and surface energy but we notice higher energy valued for structures with low porosity.

The results obtained in this work can be used as a first step to design NAA as porous hydrophobic/oleophilic material for specific purposes in particular conditions such as microfluidics or material for oil/water separation.

CRediT authorship contribution statement

Pilar Formentín: Conceptualization, Methodology, Investigation, Writing – original draft. **Laura K. Acosta:** Methodology, Investigation. **Lluís F. Marsal:** Conceptualization, Investigation, Supervision.

Declaration of competing interest

The authors declare that they have no known competing financial interests or personal relationships that could have appeared to influence the work reported in this paper.

Data availability

Data will be made available on request.

Acknowledgments

This work was supported by the Spanish Ministerio de Ciencia e Innovación (MICINN) PDI2021-128342OB-I00, and by the Catalan Institution for Research and Advanced Studies (ICREA) under the ICREA Academia Award 2021.

Appendix A. Supplementary data

Supplementary data to this article can be found online at https://doi.org/10.1016/j.matchemphys.2023.127686.

References

[1] X. Yao, Y. Song, L. Jiang, Applications of bio-inspired special wettable surfaces, Adv. Mater. 23 (2011) 719–734, https://doi.org/10.1002/adma.201002689.
[2] D. Tian, J. Zhai, Y. Song, L. Jiang, Photoelectric cooperative induced wetting on aligned-nanopore arrays for liquid reprography, Adv. Funct. Mater. 21 (2011) 4519–4526, https://doi.org/10.1002/adfm.201101008.
[3] M. Liu, L. Gan, L. Chen, Z. Xu, D. Zhu, Z. Hao, L. Chen, Supramolecular Core-Shell nanosilica@liposome nanocapsules for drug delivery, Langmuir 28 (2012) 10725–10732, https://doi.org/10.1021/la3021645.
[4] D.L. Schmidt, R.F. Brady Jr., K. Lam, D.C. Schmidt, M.K. Chaudhury, Contact angle hysteresis, adhesion and marine biofouling, Langmuir 20 (2004) 2830–2836, https://doi.org/10.1021/la3021645.
[5] C.T. Hsieh, J.M. Chen, R.R. Kuo, T.S. Lin, C.F. Wu, Influence of roughness on water- and oli-repellent surfaces coated with nanoparticles, Appl. Surf. Sci. 240 (2005) 318–326, https://doi.org/10.1016/j.apsusc.2004.07.016.
[6] L. Schneider, M. Laustsen, N. Mandsberg, R. Taborysky, The influence of structures heights and opening angles of micor- and nanocones on the macroscopic surface wetting properties, Nat. Sci. Rep. 6 (2016), 21400, https://doi.org/10.1038/srep21400.
[7] R.N. Wenzel, Resistance of solid surfaces to wetting water, Ind. Eng. Chem. 28 (1936) 988–994, https://doi.org/10.1021/ie50320a024.
[8] A.B.D. Cassie, S. Baxter, Wettability of porous surfaces, Trans. Faraday Soc. 40 (1944) 546–551, https://doi.org/10.1039/TF944000546.
[9] Z.X. Jiang, L. Geng, Y.D. Huang, Desing and fabrication of hydrophobic copper mesh with striking loading capacity and pressure resistance, J. Phys. Chem. C 114 (2010) 9370–9378, https://doi.org/10.1021/jp1009516.
[10] J.B. Boreyko, C.H. Baker, C.R. Poley, C.H. Chen, Wetting and dewetting transitions on hieraechical superhydrophobic surfaces, Langmuir 27 (2011) 7502–7509, https://doi.org/10.1021/la201587u.
[11] T. Young, An assay on the cohesion of fluids, Phil. Trans. R. Soc. B 95 (1805) 65–87, https://doi.org/10.1098/rstl.1805.0005.
[12] J. Yang, J. Wang, C.W. Wang, X. He, Y. Li, J.B. Chen, F. Zhou, Intermediate wetting states on nanopoorus structures of anodic aluminium oxide surfaces, Thin Solid Films 562 (2014) 353–360, https://doi.org/10.1016/j.tsf.2014.04.020.
[13] C. Ran, G. Ding, W. Liu, Y. Deng, W. Hou, Wetting on nanoporous alumina surface: transition between Wenzel and Cassie states controlled by surface structure, Langmuir 24 (2008) 9952–9955.
[14] L. Yao, M. Zheng, L. ma, W. Li, M. Li, W. She, Self-assembly of diverse alumina architectures and their morphology-dependent wettability, Mater. Res. Bull. 46 (2011) 1403–1408, https://doi.org/10.1016/j.materresbull.2011.05.018.
[15] D.L. Shimanovich, A.I. Vorobjova, D.I. Tishkevich, A.V. Trukhanov, M. V. Zdorovets, A.L. Kozlovskiy, Preparation and morpholy-dependent wettability of porous alumina membranes, Beilstein J. Nanotechnol. 9 (2018) 1423–1436, https://doi.org/10.3762/bjnano.9.135.
[16] A.I. Aguilar-Morales, S. Alamri, B. Voisiat, T. Kunze, A.F. Lasagni, The role of the surface nano-roughness on the wettability performance of microstructure metallic surface using direct laser interference patterning, Materials 12 (2019) 2737, https://doi.org/10.3390/ma12172737.
[17] S.S. Latthe, A.B. Gurav, C.S. Maruti, R.S. Vhatkar, Recent progress in preparation of superhydrophobic surfaces: a review, J. Surf. Eng. Mater. Adv. Technol. 2 (2012) 76–94, https://doi.org/10.4236/jsemat.2012.22014.
[18] T. Kikuchi, F. Onoda, M. Iwai, R.O. Suzuki, Influence of sub-10 nm anodic alumina nanowire morphology formed by two-step anodizing aluminum on water wettability and slipping behavior, Appl. Surf. Sci. 546 (2021), 149090, https://doi.org/10.1016/j.apsusc.2021.149090.
[19] C. Wang, R. Shao, G. Wang, J. Zhao, Z. Sha, Controllable wet etching of porous anodic alumina toward highly ordered hierarchical interfaces, Surf. Coating. Technol. 412 (2021), 127016, https://doi.org/10.1016/j.surfcoat.2021.127016.
[20] K. Senthil, G. Kwak, K. Yong, Fabrication of superhydrophobic vanadium pentoxide nanowires surface by chemical modification, Appl. Surf. Sci. 258 (2012) 7455–7459, https://doi.org/10.1016/j.apsusc.2012.04.060.
[21] J. Yong, F. Chen, Q. Yang, J. Huo, X. Hou, Superoleophobic. Surf. Chem. Soc. Rev. 46 (2017) 4168–4217, https://doi.org/10.1039/c6cs00751a.
[22] S.-Y. Li, X.-G. Xiang, B.-H. Ma, X.-D. Meng, Facile preparation of diverse alumina structures by anodization and superhydrophobic surfaces tuneable water droplet adhesion, J. Allows. Comp. 779 (2019) 219–228, https://doi.org/10.1016/j.jallcom.2018.11.222.
[23] J.G. Buijnsters, R. Zhong, N. Tsyntsaru, J.-P. Celis, Surface wettability of macroporous anodized aluminum oxide, ACS Appl. Mater. Interfaces 5 (2013) 3224–3233, https://doi.org/10.1021/am4001425.
[24] Y. Yang, L. Hong, N. Vaidyanathan, S.G. Weber, Preparation and assessment of fluorous supported liquid membranes based on porous alumina, J. Membrane. 345 (2009) 170–176, https://doi.org/10.1016/j.memsci.2009.08.042.
[25] Y. Qi, Z. Yang, W. Huang, J. Zhan, Robust, Superhydrophobic surface for anti-icing and cooling performance: application of fluorine-modified TiO_2 and fumed SiO_2, Appl. Surf. Sci. 538 (2021), 148131, https://doi.org/10.1016/j.apsusc.2020.148131.
[26] P. Formentín, L.F. Marsal, Hydrophobic/Oleophilic structures based on macroporous silicon: effect of topography and fluoroalkyl silane functionalization on wettability, Nanomaterials 11 (2021) 670, https://doi.org/10.3390/nano11030670.
[27] J. Sonogok, M. Tuominem, H. Teisala, J. Haapanen, J. Mäkelä, J. Kuusipalo, M. Toivakka, Paper-based microfluidics: fabrication, technique and dynamics of capillary-driven surface flow, ACS Appl. Mater. Interfaces 6 (2014) 20060–20066, https://doi.org/10.1021/am5055806.
[28] G.H. Kim, B.H. Lee, H. Im, S.B. Jeon, D. Kim, M.L. Seol, H. Hwang, Y.K. Choi, Controlled anisotropic wetting of scalloped silicon nanogroove, RSC Adv. 6 (2016) 41914–41918, https://doi.org/10.1039/c6ra06379a.
[29] L. Feng, Z. Zhang, Z. Mai, Y. Ma, B. Liu, L. Jiang, D. Zhu, A super-hydrophobic and super-oleophilic coating mesh film for the separation of oil and water, Angew. Chem. Int. Ed. 43 (2004) 2012–2014, https://doi.org/10.1002/anie.200353381.
[30] Y. Yu, H. Chen, Y. Liu, V. Craig, L.H. Li, Y. Chen, Superhydrophobic and superoleophilic boron nitride nanotube-coated stainless steel meshes for oil and water separation, Adv. Mater. Interfac. 1 (2014), 1300002, https://doi.org/10.1002/admi.201300002.
[31] Z. Xue, Y. Cao, N. Liu, L. Feng, L. Jiang, Special wettable materials for oil/water separation, J. Mater. Chem. 2 (2014) 2445–2460, https://doi.org/10.1039/c3ta13397d.

[32] G. Li, Z. Zhang, P. Wu, S. Wu, Y. Hu, W. Zhu, J. Li, D. Wu, X. Li, J. Chu, One-step facile fabrication of controllable microcone and micromolar silicon arrays with tunable wettability by liquid-assisted femtosecond lase irradiation, RSC Adv. 6 (2016) 37463–37471, https://doi.org/10.1039/c6ra06949e.
[33] Z. Cheng, H. Liu, H. Lai, Y. Du, K. Fu, C. Li, J. Yu, N. Zhang, K. Sun, Regulating underwater oil adhesion on superoleophobic copper films through assembling n-alkanoic acids, ACS Appl. Mater. Interfaces 7 (2015) 20410–20417, https://doi.org/10.1021/acsami.5b06374.
[34] J. Ge, Y.D. Ye, H.B. Yao, X. Zhu, X. Wang, L. Wu, J.L. Wang, H. Ding, N. Yong, L. H. He, S.H. Yu, Pumping through porous hydrophobic/oleophilic materials: an alternative technology for oil spill remediation, Angew. Chem., Int. Ed. 53 (2014) 3612–3616, https://doi.org/10.1002/anie.201310151.
[35] L. Vojkuvka, A. Santos, J. Pallarès, J. Ferré-Borrull, L.F. Marsal, J.P. Celis, On the mechanical properties of nanoporous anodized alumina by nanoindentation and sliding tests, Surf. Coating. Technol. 206 (2012) 2115–2124, https://doi.org/10.1016/j.surfcoat.2011.09.040.
[36] C. Guo, X.-W. Wang, Z.-H. Yuan, Pore diameter-dependence wettability of porous anodized aluminum oxide membranes, J. Porous Mater. 20 (2013) 673–677, https://doi.org/10.1007/s10934-012-9641-7.
[37] Y. Kim, S. Lee, H. Cho, B. Park, D. Kim, W. Hwang, Robust Superhydrophilic/Hydrophobic surface based on self-aggregated Al_2O_3 nanowires by single-step anodization and self-assembly method, ACS Appl. Mater. Interfaces 4 (2012) 5074–5078, https://doi.org/10.1021/am301411z.
[38] Y. Kim, W. Hwang, H. Cho, J.-W. Lee, A study on the minute change of the alumina surface structure according to the anodizing conditions for the production of a robust wettability-modified surfaces, Surf. Coating. Technol. 439 (2022), 128453, https://doi.org/10.1016/j.surfcoat.2022.128453.
[39] C. Chen, Y. Zuo, B. Liu, H. Xue, B. Ma, X. Li, Microstructure and wear resistance of nano titanium dioxide strengthening hardfacing material, Vacuum 162 (2019) 175–182, https://doi.org/10.1016/j.vacuum.2019.01.045.
[40] L. Skowronski, A.A. Wachowiak, W. Wachowiak, Optical and microstructural properties of decorative Al/Ti/TiO2 interference coatings, Appl. Surf. Sci. 421 (part B) (2017) 794–801, https://doi.org/10.1016/j.apsusc.2017.03.276.
[41] A. Santos, T. Kumeria, D. Losic, Nanoporous anodic alumina: a versátil platform for optical biosensors, Material (Basel) 7 (2014) 4297–4320, https://doi.org/10.3390/ma7064297.
[42] C.F. Huang, Y. Llin, Y.K. Shen, Y.M. Fan, Optimal processing for hydrophobic nanopillar polymer surfaces using nanoporous anodic alumina template, Appl. Surf. Sci. 305 (2014) 419–426, https://doi.org/10.1016/j.apsusc.2014.03.105.
[43] M.P. Montero-Rama, A. Viterisi, C. Eckstein, J. Ferré-Borrull, L.F. Marsal, In-situ removal of thick barrier layer in nanoporous anodic alumina by constant current Re-anodization, Surf. Coating. Technol. 380 (2019), 125039, https://doi.org/10.1016/j.surfcoat.2019.125039.
[44] M. Baranowska, A.J. Slota, P.J. Eravuchira, G. Macias, E. Xifré-Pérez, J. Pallarès, J. Ferré-Borrull, L.F. Marsal, Protein attachment to nanoporous anodic alumina for biotechnological applications: influence of pore size, protein size and functionalization path, Colloids Surf. B Biointerf. 122 (2014) 375–383, https://doi.org/10.1016/j.colsurfb.2014.07.027.
[45] E.E.L. Swan, K.C. Popat, T.A. Desai, Peptide-immobilized nanoporous alumina membranes for enhanced osteoblast adhesion, Biomaterials 26 (2005) 1969–1976, https://doi.org/10.1016/j.biomaterials.2004.07.001.
[46] P. Formentín, U. Catalán, L. Pol, S. Fernández-Castillejo, R. Solà, L.F. Marsal, Collagen and fibronectin Surface modofication of nanoporous anodic alumina and macroporous silicon for endotelial cell cultures, J. Biol. Eng. 12 (2018) 21, https://doi.org/10.1186/s13036-018-0111-x.
[47] E. Xifré-Pérez, S. Guaita-Esteruelas, M. Baranowska, J. Pallarès, L. Masana, L. F. Marsal, ACS Appl. Mater. Interfaces 7 (2015) 18600–18608, https://doi.org/10.1021/acsami.5b05016.
[48] M. Aramesh, J. Cervenka, Surface modification of porous anodic alumina for medical and biological applications, in: Deepak M. kalaskar (Ed.), Alexander Seifalian, achala de Mel, Nanomedicine, One Central Press (OCP), 2014, pp. 439–467.
[49] M. Porta-Batalla, C. Eckstein, E. Xifré-Pérez, P. Formentín, J. Ferré-Borrull, L. F. Marsal, Sustained, controlled and stimuli-responsive drug reléase systems base don nanoporous anodic alumina with layer-by-layer polyelectrolite, Nanoscale Res. Lett. 11 (2016) 1–9, https://doi.org/10.1186/s11671-016-1585-4.
[50] A. Ressine, D. Finnskog, G. Marko-Varga, T. Laurell, Superhydrophobic properties of nanostructured-microstructured porous silicon for improved surface-based bioanalysis, NanoBiotechnology 4 (2008) 18–27.
[51] M. Pei, L. Huo, K. Zhang, H. Zhou, P. Liu, Hydrophobic surface via coating fluorinated homopolymer: effects of the surface etching of silicon wafer and coated fluoropolymer amount, Colloids Surf., A 585 (2020), 123984, https://doi.org/10.1016/j.colsurfa.2019.123984.
[52] A. Santos, J. Ferré-Borrull, J. Pallarès, L.F. Marsal, Hierarchical nanoporous anodic alumina templates by asymmetric two-step anodization, Phys. Status Solidi A 3 (2011) 668–674, https://doi.org/10.1002/pssa.201026435.
[53] J. Ferré-Borrull, J. Pallarès, G. Macías, L.F. Marsal, Nanostructural engineering of nanoporous anodic alumina for biosensing applications, Materials 7 (2014) 5225–5253, https://doi.org/10.3390/ma7075225.
[54] A. Santos, L. Vojkuvka, M. Alba, V.S. Balderrama, J. Ferré-Borrull, J. Pallarès, L. F. Marsal, Understanding and morphology control of pore modulations in nanoporous alumina by discontinuos anodization, Phys. Stats Solidi A 10 (2012) 2045–2048, https://doi.org/10.1002/pssa.201228150.
[55] M. Norek, A. Krasinki, Controlling of water wettability by structural and chemical modification of porous anodic alumina (PAA): towards super-hydrophobic surfaces, Surf. Coating. Technol. 276 (2015) 464–470, https://doi.org/10.1016/j.surfcoat.2015.06.028.
[56] D.L. Shimanovich, A.I. Vorobjova, D.I. Tishkevich, A.V. Trukhanov, M.V. dorovets, A.L. Kozlovskiy, Preparation and morphology-dependent wettability of porous alumina membranes, Beilstein J. Nanothechnol. 9 (2018) 1423–1436, https://doi.org/10.3762/bjnano.9.135.
[57] G.-O. Kim, H. Lee, E. Ma, C. Kang, Y.-U. Kwon, Viability studies of cells on nanostructured surfaces with various feature sizes, Bull. Kor. Chem. Soc. 38 (2017) 1447–1454, https://doi.org/10.1002/bkcs.11325.
[58] S. Kim, A.A. Polycarpou, H. Liang, Electrical-potential induced surface wettability of porous metallic nanostructures, Appl. Surf. Sci. 351 (2015) 460–465, https://doi.org/10.1016/j.apsusc.2015.05.148.
[59] H.-J. Wang, Y.-Y. Sun, Y. Cao, K. Wang, L. Yang, Y.-D. Zhang, Z. Zheng, Is there an optimal topographical surface in nano-scale affecting protein adsorption and cell behaviors? Part II, J. Nanoparticle Res. 14 (2012) 862, https://doi.org/10.1007/s11051-012-0862-0.
[60] C.J. van Oss, M.K. Chaudhury, R.J. Good, Interfacial Lifshitz-van der Waals and polar interactions in macroscopic systems, Chem. Rev. 88 (1988) 927–941.
[61] C.J. Oss, Interfacial Forces in Aqueous Media, second ed., CRC Press, Atlanta, G.A., U.S.A., 2006. New York: marcel Dekker 1994.
[62] L.K. Koopal, Wetting of solid surfaces: fundamentals and charge effects, Adv. Colloid Interface Sci. 179–182 (2012) 29–42, https://doi.org/10.1016/j.cis.2012.06.009.
[63] N. Arsalan, J.J. Buiting, Q.P. Nguyen, Surface energy and wetting behavior of reservoir rocks, Colloids Surf., A 467 (2015) 107–112, https://doi.org/10.1016/j.colsurfa.2014.11.024.